Protein transport via the cpTat pathway displays cooperativity and is stimulated by transport-incompetent substrate

Natahan N. Alder[1], Steven M. Theg*

Division of Biological Sciences, Section of Plant Biology, University of California, One Shields Avenue, Davis, CA 95616, USA

Abstract Kinetic analyses of cpTat-mediated protein transport across the thylakoid membrane were conducted, revealing three important characteristics of this translocation pathway. First, transport via the cpTAT system displays a non-Michaelis–Menten, sigmoidal rate–substrate relationship with an apparent Hill coefficient of 1.80, indicative of positive homotropic cooperativity. Second, the presence of transport-incompetent substrates was found not to competitively inhibit the translocation of transport-competent substrates. However, the presence of low concentrations of transport-incompetent protein enhances the transport of wild type substrate. Together, these findings suggest that interaction between Tat machinery components and both transport-competent and transport-incompetent protein may elicit a cooperative effect on the translocation rate.
© 2003 Published by Elsevier Science B.V. on behalf of the Federation of European Biochemical Societies.

Key words: cpTat pathway; Thylakoid; Kinetics; Cooperativity

1. Introduction

Among protein translocation systems, the Tat pathway is unusual in that it requires neither *cis*-soluble factors nor nucleoside triphosphate hydrolysis to mediate transport, but rather relies strictly on a transmembrane protonmotive force (pmf) as an energetic source [1–3]. Moreover, the Tat machinery is capable of transporting fully folded substrates across energy conserving membranes [4–7]. Two homologous Tat pathways have been characterized: the bacterial Tat system, which exports proteins across the inner membrane of gram negative bacteria into the periplasm, and the cpTAT (ΔpH-dependent) system of chloroplasts, which transports nuclear encoded proteins across the thylakoid membrane into the lumen. In *Escherichia coli*, the components of the Tat system are encoded by the *tat* operon (*tatA*, *tatB*, and *tatC*), and by the monocistronic *tatE* [8–10]. Orthologous genes in plants include *hcf106* (*tatB*), *tha4* (*tatA*), and *cptatC* (*tatC*) [11–14]. Presently, these are the only components found to comprise the large (ca. 600–700 kDa) Tat complexes in thylakoids [12,15,16] and in bacteria [17,18].

In vitro assays of substrate transport into isolated thylakoids have resolved cpTat-mediated translocation into a two-step process. The first step entails the reversible binding of precursor substrate to a complex composed of cpTatC and Hcf106 [16,19,20]. This step occurs independently of the ΔpH, and results in the formation of a productive bound intermediate, which is specifically competed by cpTAT substrates [20]. The second step is the ΔpH-dependent translocation of bound substrates across the membrane, a step which requires the association of Tha4 with the cpTatC–Hcf106 receptor complex [16,21].

Substrates of the Tat pathway contain a conserved twin-arginine (RR) motif in the signal peptide, which is essential for transport [22–24], and alteration of this motif renders Tat substrates non-transportable in thylakoids [22,23,25], and in bacteria [26–28]. However, the potential effects of such RR mutant proteins on cpTat-mediated transport of wild type substrate has not been addressed. For example, features of the transit peptide other than the RR motif, or motifs within the mature protein itself, may allow limited engagement of the machinery without allowing for complete translocation. In the present study, these possibilities were addressed by conducting competitive inhibition experiments with mutant cpTat substrates. This analysis revealed three important features of the cpTat pathway. First, cpTat-mediated transport displays sigmoidal saturation kinetics indicative of positive homotropic cooperativity. Second, constructs with alterations in the RR motif do not competitively inhibit transport of wild type substrate, indicating that they do not engage the machinery at a kinetically limiting step. Finally, the presence of low concentrations of mutant signal peptide-bearing substrate appeared to enhance the transport efficiency of wild type substrate, suggesting limited mutant-machinery interaction at a point upstream of the translocation (RR-requiring) step.

2. Material and methods

2.1. Production of substrate protein

The preparation of genes encoding the wild type intermediate maize OE17 (iOE17 WT), the R14K R15K mutant (iOE17 KK), the R14Q R15Q mutant (iOE17 QQ), and the mature OE17 (mOE17), each bearing a C-terminal 6×His tag, and their incorporation into the IPTG-inducible pET23a (Novagen) vector is described in [29]. Plasmids used for overexpression were introduced into *E. coli* strain BL21-CodonPlus™ (DE3)-RIL [F⁻ *ompT hsdS* (r$_B^-$ m$_B^-$) *dcm⁺* Tet^r *galλ* (DE3) *endA* Hte [*argU ileY leuW* Cam^r]] (Stratagene) via electroporation. The overexpression and Ni-NTA affinity purification of ³H-radiolabeled (iOE17 WT only) or non-radiolabeled (all constructs) proteins was conducted exactly as in [29]. Proteins were stored in 8 M

*Corresponding author.
E-mail address:* smtheg@ucdavis.edu (S.M. Theg).

[1] Present address: Department of Medical Biochemistry and Genetics, Texas A&M University System Health Science Center, College Station, TX 77843-1114, USA.

urea and 100 mM K$^+$-Tricine, pH 8.0 at −80°C for no longer than 1 week prior to use.

2.2. Thylakoid preparation and protein transport assays

Chloroplasts were isolated from 9 to 12 day old pea seedlings and osmotically lysed to obtain thylakoids as described [30], and thylakoids were stored in import buffer (IB; 50 mM K$^+$-Tricine, pH 8.0, 330 mM sorbitol, 5 mM MgCl$_2$) on ice in the dark.

In vitro protein transport assays included indicated concentrations of radiolabeled substrate, non-radiolabeled protein, and thylakoids (0.33 mg chlorophyll ml^{-1}) in IB at a volume of 60 µl. Prior to transport measurements, all protein stocks were diluted to identical concentrations, such that the final [urea] was identical for a given set of experiments, and ranged from 43 to 57 mM for all assays reported. This concentration range of urea has been shown to have no effect on thylakoid protein transport [19,31]. Reactions were placed in front of an IR-filtered actinic light source for 12 min, followed by protease digestion of non-transported protein and preparation of samples for SDS–PAGE and fluorography as described [29]. Fluorograms were calibrated by simultaneous exposure with a gel strip containing a concentration series of radiolabeled protein.

2.3. Data analysis

Protein transport as a function of time was quantified from fluorograms using NIH Image, and data were fitted using Kaleidagraph software. Time course data (Fig. 1A) were fit to an irreversible two-step mechanism (free protein $\xrightarrow{k_1}$ bound protein $\xrightarrow{k_2}$ transported protein) as follows:

$$v = V_{max}\left[1 - \left(\frac{k_1}{k_2 - k_1}\right)e^{-k_1 t} - \left(\frac{k_2}{k_1 - k_2}\right)e^{-k_2 t}\right], \quad (1)$$

in which k_1 and k_2 represent first-order rate constants, and v and V_{max} correspond to the measured and maximal transport rates, respectively. Data from velocity vs. [substrate] curves were fitted according to the Hill equation:

$$v = \frac{V_{max}[S]^n}{[S]^n + K_m}, \quad (2)$$

in which [S] is the substrate (^{3}H iOE17) concentration, K_m is the apparent affinity constant, and n is the Hill coefficient. When $n = 1$, this equation reduces to the Henri–Michaelis–Menten equation [32].

For determination of n, Eq. 2 is converted into the logarithmic form:

$$\log\left(\frac{v}{V_{max} - v}\right) = n \log[S] - \log K_m, \quad (3)$$

whereby n is read from the slope of a plot of $\log[v/(V_{max}-v)]$ versus $\log[S]$.

3. Results

3.1. Protein transport along the cpTat pathway shows sigmoidal saturation kinetics

Throughout the following kinetic analysis, we monitored the transport radiolabeled, overexpressed iOE17 WT, a native cpTat substrate, into isolated thylakoids. The extent of transport was quantified as the amount of processed, protease protected protein following a transport reaction. Time course analyses of cpTat-mediated transport revealed biphasic kinetics (Fig. 1A, solid line) as shown previously [19,29,31,33], which can be modeled as an irreversible, two-step, first-order reaction (Eq. 1). The first step, indicated by the initial lag phase, likely represents the energy-independent establishment of bound translocation intermediates on the pathway via protein–protein interactions [16,19,20]. Notably, this lag phase is removed by pre-incubation of thylakoids with substrate followed by a transport chase in the presence of a ΔpH [19]. The second step, pmf-dependent transport monitored by the appearance of mature substrate, displays saturation, which likely
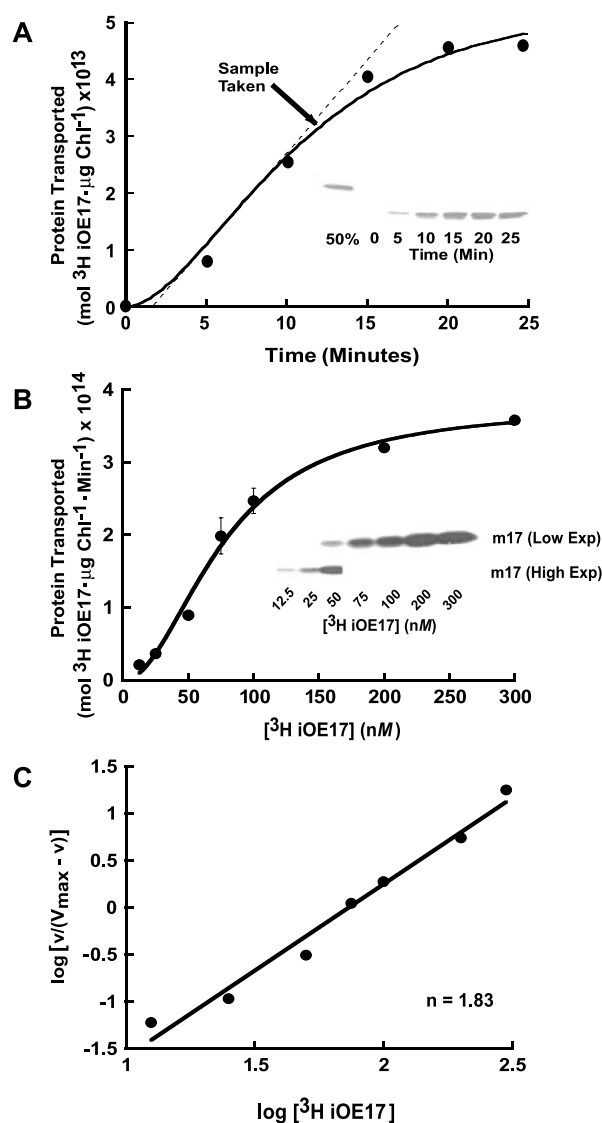

Fig. 1. Kinetic analysis of ^{3}H iOE17 transport into isolated thylakoids. A: Time course of ^{3}H iOE17 transport. Isolated thylakoids were incubated with 200 nM ^{3}H iOE17 in the light for the assay times indicated (●). The solid line is a fit of measured points to an irreversible two-step first-order reaction mechanism [35], and the dashed line indicates the slope of the tangent to the inflection point, indicating the linear phase of transport (12 min). In this biphasic transport course, the minimal time for maturation is 2.0 min, and the maximum rate of transport is 250 proteins thylakoid^{-1} s^{-1}. The inset shows the fluorogram from which the data were quantified, indicating 50% of the ^{3}H iOE17 added (6×10^{-12} mol), followed by the mature-sized, protease-protected protein transported over the times shown. B: Velocity-substrate analysis of ^{3}H iOE17 transport. 12-min transport reactions were conducted with thylakoids and 12.5–300 nM ^{3}H iOE17. Each point (●) represents a mean of four measurements, with the indicated standard errors. The solid line is a sigmoidal fit to the data (Eq. 2) from least squares analysis ($R = 0.99$) with $V_{max} = 3.78 \times 10^{-14}$ mol ^{3}H iOE17 µg chlorophyll^{-1} min^{-1}, $K_m = 76.6$ nM, and $n_{app} = 1.8$. The inset shows representative fluorograms of low exposure for higher substrate concentrations ([^{3}H] iOE17 = 50–300 nM), and high exposure for lower substrate concentrations ([^{3}H] iOE17 = 12.5–50 nM). Standard lanes (data not shown) were included in each exposure for quantitation. B: Hill plot of ^{3}H iOE17 transport. Data from (B) were transformed according to Eq. 3 to yield a linear Hill plot, revealing a slope of 1.83 ($= n_H$).

corresponds to the depletion of translocation-competent protein. The energy- and substrate-dependent assembly of the translocon [21] is probably between the first and second steps described here, and appears not to be kinetically limiting under our experimental conditions. The maximum rate of transport is observed after 12 min, which corresponds to the position of the inflection point of the fitted curve (Fig. 1, dashed line). Because the transport rate is linear out to 12 min for all substrate concentrations examined (data not shown), measurements at this time point provide reasonable representations of v_o, and accordingly may therefore be used in Michaelis–Menten analyses, even though a significant proportion of substrate has been utilized by this point.

We then characterized the substrate concentration versus velocity relationship of cpTat-mediated protein transport (Fig. 1B). Due to the wide substrate range of this analysis ([^{3}H iOE17] = 12.5–300 nM), two separate exposures of fluorograms were required to accurately quantify the data: a short exposure for high [S], and a longer exposure for low [S] (inset, Fig. 1B). Surprisingly, a sigmoidal saturation profile, rather than a hyperbolic one, was generated (Fig. 1B, solid line). A sigmoidal fit to the data revealed a V_{max} of 3.78×10^{-14} mol ^{3}H iOE17 µg chlorophyll^{-1} min^{-1}, a $K_{0.5}$ of 76.6 nM, and an apparent Hill coefficient (n_{app}) of 1.80. These data are recast in a Hill plot in Fig. 1C, from which the slope indicates an n_H value of 1.83.

3.2. Non-transportable substrates do not competitively inhibit transport via the cpTat pathway

It is well established that alteration of the requisite RR motif in the signal sequence of Tat substrates renders the substrate non-transportable both in chloroplasts [22,24,25], and in bacteria [26–28]. However, whether non-transportable substrates competitively inhibit transport along the Tat pathway has not been determined. To address this question, iOE17 constructs were created in which the RR motif was converted to a KK (iOE17 KK), QQ (iOE17 QQ, see below), or in which the transit sequence was removed completely (mOE17) [29]. The transport rate of 12.5–400 nM ^{3}H iOE17 was measured in the presence of 100 nM of these transport-incompetent proteins, or with an equal volume of protein buffer (Fig. 2).

The presence of iOE17 KK or mOE17 had little or no effect on cpTat-mediated transport of ^{3}H iOE17, as the saturation curves with these potential competitor proteins were not different from the control curve. In contrast, as expected, the presence of 100 nM non-radiolabeled iOE17 WT resulted in competitive inhibition of radiolabeled substrate transport, as the measured V_{max} did not differ from the control, but the $K_{0.5}$ was significantly increased. From this analysis, non-labeled iOE17 shows an apparent inhibition constant of 46 nM. Taken together, these results indicate that not only does alteration of the RR or removal of the transit sequence render cpTat substrate non-transportable, but further, that such protein does not interact with the translocation machinery in a kinetically limiting step.

3.3. The presence of non-transportable protein enhances cpTat-mediated translocation of transport-competent substrate

The apparent positive cooperatively observed in the velocity curves of this study (Figs. 1 and 2) suggests that the binding of substrate to one site may increase the affinity of a coupled site, thereby enhancing transport efficiency. It follows that
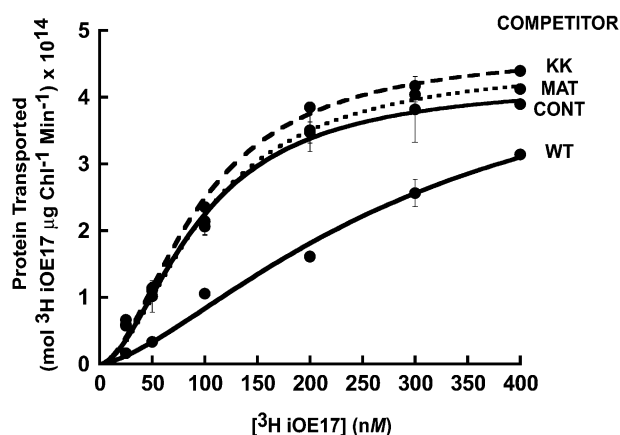

Fig. 2. Competitive inhibition analysis. Transport reactions were conducted with 25–400 nM ^{3}H iOE17 in the presence of either 100 nM non-radiolabeled competing protein (WT, KK, MAT), or an equal volume of protein buffer (CONT). Each point (●) represents a mean of two measurements, with the indicated standard errors. Sigmoidal fits to the data and Hill plot analysis indicate V_{max} values of 4.24, 5.08, 4.73, and 4.52×10^{-14} mol ^{3}H iOE17 µg chlorophyll^{-1} min^{-1} and K_m values of 93.7, 297.2, 94.4, and 100.5 nM for CONT, WT, KK, and MAT samples, respectively.

addition of an allosteric effector to a reaction in which the substrate concentration is in the rapidly rising phase of the sigmoidal curve should result in a measurable increase in transport rate. We asked whether non-transportable substrates could act as such allosteric effectors. To this end, the transport of 25 nM ^{3}H iOE17 was monitored in the presence of increasing concentrations of unlabeled protein (up to 50 nM WT, KK, QQ, or MAT) to determine whether transport efficiency was enhanced (Fig. 3). Measured transport rates (Fig. 3B) were normalized relative to control conditions (no unlabeled protein; dashed lines), and the data points indicate the change in transport efficiency with increasing unlabeled protein concentration.

As expected, the addition of increasing concentrations of non-radiolabeled iOE17 WT (acting as a competitive inhibitor) resulted in progressive reduction in transport of ^{3}H iOE17. However, addition of the non-transportable substates iOE17 KK and iOE17 QQ resulted in significantly enhanced transport rates of ^{3}H iOE17 relative to control conditions. By comparison, the addition of mOE17 to reactions had relatively little effect on ^{3}H iOE17 transport. These results suggest that transit peptide-bearing substrates which are not competent for transport interact with the cpTat machinery in a way that enhances efficiency, possibly by the same mechanism which results in the observed positive cooperativity. While we acknowledge that the presence of modified Tat substrate could enhance ^{3}H iOE17 transport by non-specific effects (e.g. by stabilizing the low concentrations of substrate protein present), we note that this phenomenon is transit peptide-dependent, suggesting a bona fide interaction between variant constructs and the Tat machinery.

One possible explanation for the apparent cooperativity we observe is that substrates must dimerize before transport, as shown for thiolase transport into peroxisomes [34]. To this end, we tested whether radiolabeled transport-incompetent protein (iOE17 KK or mOE17) was co-translocated with non-radiolabeled iOE17 WT, and obtained no evidence for this mechanism (data not shown). We conclude that either
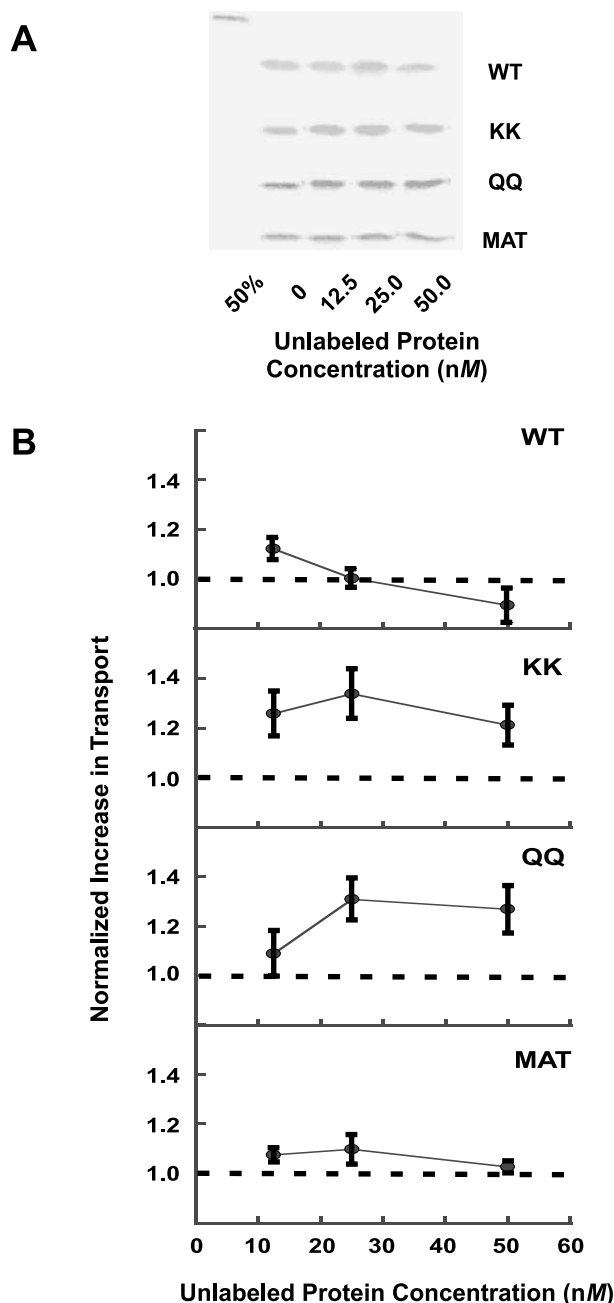
Fig. 3. Enhancement of ^{3}H iOE17 transport by non-transportable protein. Transport reactions were conducted as above with 25 nM ^{3}H iOE17 in the presence of 0, 12.5, 25, and 50 nM non-radiolabeled protein (WT, KK, QQ, MAT). A: Representative fluorograms of ^{3}H iOE17 transport in the presence of the indicated concentrations of unlabeled protein. B: Quantitation of ^{3}H iOE17 transport. For each concentration series, the change in transport relative to the buffer only control is shown, and the means of those values (●) are reported ($n = 8$ for WT, KK; $n = 4$ for QQ, MAT) with the indicated standard errors. The dashed line indicates the point on the ordinate reflecting the control level of transport.

dimerization of Tat substrates is not responsible for the cooperative nature of the kinetics, or, less likely, that the competent signal peptide is responsible for transport-enabling dimerization.

If the cooperativity observed with transport-incompetent precursors results from their mediating the assembly of an active Tat translocon, and if this assembly step is rate limiting,

it is possible that preincubation of thylakoids with such precursors prior to addition of competent substrates might eliminate the characteristic lag phase (Fig. 1A), as seen after preincubation with wild type substrate [19]. To test this, we preincubated thylakoids in the dark with 100 nM iOE17 KK, followed by an in vitro transport time course of 100 nM ^{3}H iOE17. However, transport under these conditions resulted in a biphasic time course, exactly as in Fig. 1 (data not shown). We therefore conclude that the cooperative effect observed with non-transportable proteins does not result in elimination of rate-limiting step in which bound intermediates are formed.

4. Discussion

This study addressed the kinetic characteristics of cpTat-mediated protein translocation, as well as potential interaction of non-transportable protein with the cpTat machinery. Protein transport via the cpTat pathway displays a sigmoidal rate–substrate relationship (Fig. 1), indicative of allosteric proteins in which the binding of substrate to one site alters the binding affinity of another coupled site(s). A n_H of 1.8 may result from two binding sites per translocon with strong cooperativity, or multiple binding sites with weak cooperativity. It is perhaps not surprising that transport along the cpTat system obeys non-Michaelis–Menten kinetics. The cpTat binding complex is composed of a multiple cpTat-Hcf106 heterodimers to which substrates bind [16]. The results of the present study suggest that these multiple binding sites may be allosterically coupled, such that the binding of one substrate molecule increases the binding affinity of a coupled site. Alternatively, the binding of one substrate molecule may facilitate the next step in complex assembly (e.g. recruitment of Tha4 to the Hcf106–cpTatC receptor complex), consistent with the recent observation of repeated cycles of ΔpH-triggered translocon assembly and disassembly [21]. In such a scenario, the transport rate would be enhanced after binding one substrate molecule because the next molecule engages a complex that is primed for translocation. One potential advantage of such a cooperative system is that a sigmoidal rate–substrate response provides a more sensitive control over reaction rate at intermediate substate concentration than does a hyperbolic response, effectively toggling between active and non-active states over a relatively narrow substrate range. As it has been demonstrated that cpTat transport is coupled with substantial H$^+$ counterflux from the lumem [29], this sigmoidal 'switch' may act as an intrinsic regulator to conserve the ΔpH when the substrate concentration is below a particular threshold level.

The next phase of this study addressed the nature of the interaction between non-transportable protein (iOE17 KK/QQ, and mOE17) and the cpTat transport machinery. Substrates with alterations to the RR motif did not competitively inhibit transport of radiolabeled transportable substrates (Fig. 2). This is consistent with recent evidence that RR mutants do not bind stably to the cpTatC–Hcf106 complex [16], and indicates that RR mutants do not interact with the machinery during a kinetically limiting step.

On the other hand, some interaction of these mutant substrates with the transport machinery is evidenced by our observation that the presence of low concentrations of non-transportable transit peptide-bearing substrates increased the

transport rate of wild type substrate (Fig. 3). This suggests that the iOE17 KK and QQ mutants, although transport-in-competent and unable to competitively inhibit transport, may nonetheless engage the cpTat machinery in a way such that transport efficiency is increased. Further, it is possible that the mode of action by which the KK and QQ mutants exert this stimulatory effect is responsible for the apparent cooperativity observed with native iOE17 transport. That these mutants could have some limited interaction with the cpTat machinery is not entirely unexpected, as the iOE17 KK and QQ mutants have been shown to cause a reduction in the steady state ΔpH when introduced into a suspension of isolated thylakoids [29]. It is noteworthy in this context that the assembly step was seen to require a ΔpH [21]. We are aware, however, that we have not demonstrated that the H^+ flux caused by the mutant proteins is through the cpTat machinery. Future experiments comparing the effect of substrates of other pathways (e.g. proteins with Sec-type signal sequences) on the transport of low concentrations of Tat substrates will be useful in elucidating the nature of this phenomenon.

References

[1] Mould, R.M. and Robinson, C. (1991) J. Biol. Chem. 266, 12189–12193.
[2] Cline, K., Ettinger, W.F. and Theg, S.M. (1992) J. Biol. Chem. 267, 2688–2696.
[3] Klösgen, R.B., Brock, I.W., Hermann, R.G. and Robinson, C. (1992) Plant Mol. Biol. 18, 1031–1034.
[4] Clark, S.A. and Theg, S.M. (1997) Mol. Biol. Cell 8, 923–934.
[5] Hynds, P.J., Robinson, D. and Robinson, C. (1998) J. Biol. Chem. 273, 34848–34874.
[6] Thomas, J.D., Daniel, R.A., Errington, J. and Robinson, C. (2001) Mol. Microbiol. 39, 47–52.
[7] Santini, C.-L. et al. (2001) J. Biol. Chem. 276, 8159–8164.
[8] Sargent, F., Bogsh, E., Stanley, N.R., Wexler, M., Robinson, C., Berks, B.C. and Palmer, T. (1998) EMBO J. 17, 3640–3650.
[9] Bogsh, E., Sargent, F., Stanley, N.R., Berks, B.C., Robinson, C. and Palmer, T. (1998) J. Biol. Chem. 273, 18003–18006.
[10] Sargent, F., Stanley, N.R., Berks, B.C. and Palmer, T. (1999) J. Biol. Chem. 274, 36073–36082.
[11] Settles, M.A., Yonetani, A., Baron, A., Bush, D.R., Cline, K. and Martienssen, R. (1997) Science 278, 1467–1470.
[12] Mori, H., Summer, E.J., Fincher, V. and Cline, K. (1999) J. Cell Biol. 146, 45–55.
[13] Walker, M.B., Roy, L.M., Coleman, E., Voelker, R. and Barkan, A. (1999) J. Cell Biol. 147, 267–275.
[14] Mori, H., Summer, E.J. and Cline, K. (2001) FEBS Lett. 501, 65–68.
[15] Berghöfer, J. and Klösgen, R.B. (1999) FEBS Lett. 460, 328–332.
[16] Cline, K. and Mori, H. (2001) J. Cell Biol. 154, 719–729.
[17] Bolhuis, A., Bogsh, E.G. and Robinson, C. (2000) FEBS Lett. 472, 88–92.
[18] Sargent, F., Gohlke, U., de Leeuw, E., Stanley, N.R., Palmer, T., Saibil, H.R. and Berks, B.C. (2001) Eur. J. Biochem. 268, 3361–3367.
[19] Musser, S.M. and Theg, S.M. (2000) Eur. J. Biochem. 267, 2588–2598.
[20] Ma, X. and Cline, K. (2000) J. Biol. Chem. 275, 10016–10022.
[21] Mori, H. and Cline, K. (2002) J. Cell Biol. 157, 205–210.
[22] Chaddock, A.M., Mant, A., Karnauchov, I., Brink, S., Hermann, R.G., Klösgen, R.B. and Robinson, C. (1995) EMBO J. 14, 2715–2722.
[23] Berks, B.C. (1996) Mol. Microbiol. 22, 393–404.
[24] Henry, R., Carrigan, M., McCaffrey, M., Ma, X. and Cline, K. (1997) J. Cell Biol. 136, 823–832.
[25] Schnell, D.J. (1998) Annu. Rev. Plant Physiol. Plant Mol. Biol. 49, 97–126.
[26] Halbig, D., Wiegert, T., Blaudeck, N., Freudl, R. and Sprenger, G.A. (1999) Eur. J. Biochem. 263, 543–551.
[27] Cristóbal, S., deGier, J.-W., Nielsen, H. and von Heijne, G. (1999) EMBO J. 18, 2982–2990.
[28] Stanley, N.R., Palmer, T. and Berks, B.C. (2000) J. Biol. Chem. 275, 11591–11596.
[29] Alder, N.A. and Theg, S.M. (2003) Cell 112, 231–242.
[30] Cline, K., Werner-Washburne, M., Lubben, T.H. and Keegstra, K. (1985) J. Biol. Chem. 260, 3691–3696.
[31] Teter, S.A. and Theg, S.M. (1998) Proc. Natl. Acad. Sci. USA 95, 1590–1594.
[32] Segel, E. (1975) Enzyme Kinetics, John Wiley and Sons, Inc., New York.
[33] Brock, I.W., Mills, J.D., Robinson, D. and Robinson, C. (1995) J. Biol. Chem. 270, 1657–1662.
[34] Glover, J.R., Andrews, D.W. and Rachubinski, R.A. (1994) Proc. Natl. Acad. Sci. USA 91, 10541–10545.
[35] Capellos, C. and Bielski, B.H.J. (1980) Kinetic Systems, Robert E. Krieger, Huntington, NY.